

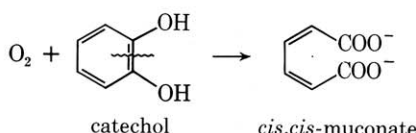
# Spectroscopic Studies of the Catechol Dioxygenases

Lawrence Que, Jr.

University of Minnesota, Minneapolis MN 55455

The catechol dioxygenases are bacterial iron-containing enzymes that catalyze the oxidative cleavage of catechols (1). These enzymes serve as a component of nature's mechanism for degrading aromatic compounds in the environment (2). The elucidation of the novel substrate activation mechanism (3) for this reaction has come about as a result of spectroscopic investigations on the enzymes coupled with comparative studies of model compounds. Central to these studies has been the phenolate-to-Fe(III) charge transfer transition which persists in all the enzyme complexes and determines the UV-visible, resonance Raman, and paramagnetic NMR properties of the iron complex in these enzymes (4).

The catechol dioxygenases catalyze the reaction shown below



In the process of cleaving the C1-C2 bond of the catechol, the enzyme incorporates the elements of dioxygen into the product (5), thus the term dioxygenase for describing the enzyme. The two best-studied examples are catechol 1,2-dioxygenase (CTD) and protocatechuate(3,4-dihydroxybenzoate) 3,4-dioxygenase (PCD). CTD, from *Pseudomonas arvillae* grown on benzoate as its sole carbon source, has a molecular weight of 63,000 with two nonidentical subunits ( $\alpha\beta Fe$ ) (5). PCD, from *Pseudomonas aeruginosa* which utilizes 4-hydroxybenzoate as its sole carbon source, has a molecular weight of 783,000 and a composition of  $(\alpha_2\beta_2 Fe)_8$  (7, 8). This enzyme has been crystallized and an X-ray diffraction study

is in progress (9).

The catechol dioxygenases are neither heme proteins nor iron sulfur proteins; the iron center is simply coordinated to ligands on the polypeptide chain. EPR and Mossbauer spec-

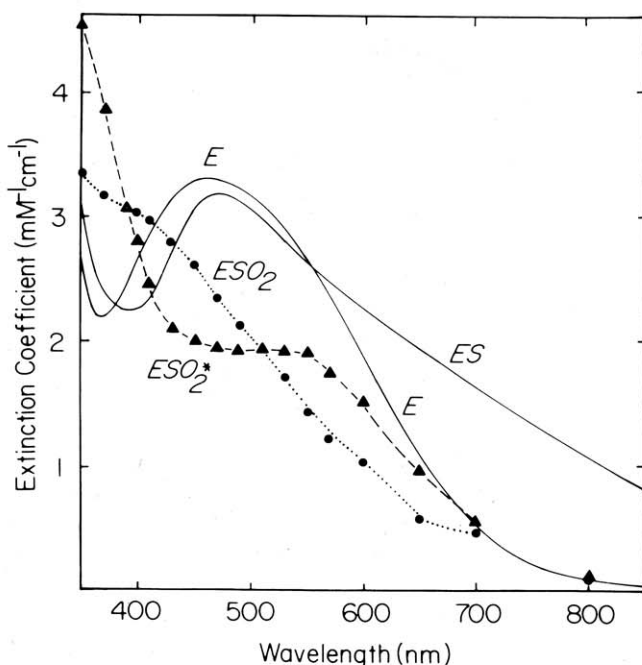


Figure 1. Visible absorption spectra of protocatechuate 3,4-dioxygenase complexes: E, native enzyme; ES, enzyme-substrate complex; ESO<sub>2</sub>, first intermediate; ESO<sub>2</sub><sup>\*</sup>, second intermediate.

troscopies have shown the native enzymes to contain a high-spin ferric center (10–12). EPR spectroscopy, which probes paramagnetic states of the metal center, reveals a signal at  $g = 4.3$  for these enzymes, characteristic of a high spin ferric center in a rhombic environment (13). Mossbauer spectroscopy probes the nuclear states of  $^{57}\text{Fe}$  center and reveals spectral parameters for the enzymes consistent with a high-spin ferric oxidation state (10–12). The enzymes are most easily characterized by visible spectroscopy which shows a broad absorption band with a maximum near 460 nm and a molar extinction coefficient of 3000–4000 per iron (Fig. 1) (1). Since ligand-field bands of high-spin ferric ions are both spin and orbitally forbidden and thus have small extinction coefficients ( $0.1\text{--}1 M^{-1}\text{cm}^{-1}$ ), the visible absorption band has been assigned to a ligand-to-metal charge transfer transition. Considering the possible amino acid ligating groups, the two with high-lying filled orbitals to serve as donor orbitals are thiolate (cysteine) and phenolate (tyrosine). Indeed, early studies favored the description of the dioxygenases as iron-sulfur proteins (16) because of EPR and visible spectral similarities to rubredoxin, a protein with a ferric center tetrahedrally coordinated to four thiolate groups.

Resonance Raman spectroscopy is an excellent technique for probing charge-transfer transitions. Raman spectroscopy provides vibrational information by measuring the energy of inelastically scattered light from a sample; the difference in the energies of the incident and scattered radiation corresponds to vibrational transitions. Normal Raman scattering is weak and thus usually impractical for dilute biologi-

cal samples. However, if the incident radiation approaches the energy of an allowed electronic transition, such as a charge transfer band, the vibrational modes that are vibronically coupled to the electronic transition will be enhanced by factors of  $10^2$ – $10^6$ , depending on the molar extinction coefficient of the transition. When the dioxygenases are probed with radiation within their absorption envelopes, resonance-enhanced Raman features at  $\sim 1170$ , 1270, 1500, and  $1600\text{ cm}^{-1}$  are observed (17–21). These have been identified as characteristic vibrations of tyrosinate, thus the assignment of the visible band as tyrosinate-to-Fe(III) charge transfer. Based on a normal mode analysis (22), the vibrations have been assigned as principally  $\delta_{\text{C-H}}$ ,  $\nu_{\text{C-O}}$ , and two  $\nu_{\text{C-C}}$ 's, respectively. In contrast, iron-sulfur proteins exhibit Raman features near 370 and  $800\text{ cm}^{-1}$ , corresponding to  $\nu_{\text{Fe-S}}$  and  $\nu_{\text{C-S}}$ , respectively (23).

The dioxygenase Raman spectrum is nicely reproduced by a model complex,  $\text{Fe}(\text{salen})(\text{OC}_6\text{H}_4\text{-4-CH}_3)$ , the *p*-cresolate serving as the tyrosinate analog (Fig. 2) (4). The *p*-cresolate vibrations, readily identified by isotopic substitution experiments, correspond well to the assigned tyrosinate vibrations. In addition, the model complex exhibits features that arise from salen vibrations, due to the presence of a salen-to-Fe(III) charge-transfer transition. The two transitions can be deconvoluted by an excitation profile study. Such a study involves obtaining Raman spectra at several wavelengths and determining the resonance enhancements of the various features relative to a standard which is not resonance enhanced. Features will exhibit greater or smaller enhancements depending on the extinction coefficient of their re-

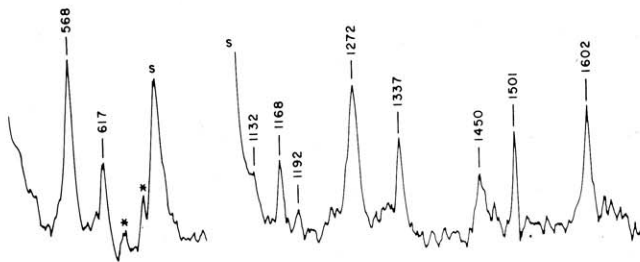


Figure 2. Resonance Raman spectrum of  $\text{Fe}(\text{salen})(\text{OC}_6\text{H}_4\text{-4-CH}_3)$  in  $\text{CD}_3\text{CN}$  with 647.1 nm excitation. Features marked S are solvent vibrations.

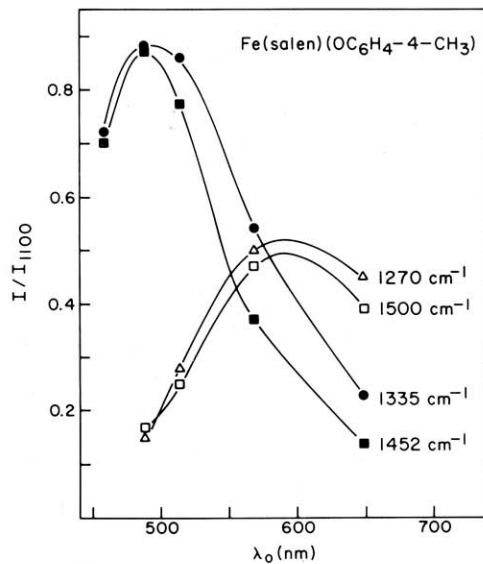


Figure 3. Excitation profile of  $\text{Fe}(\text{salen})(\text{OC}_6\text{H}_4\text{-4-CH}_3)$  vibrations.

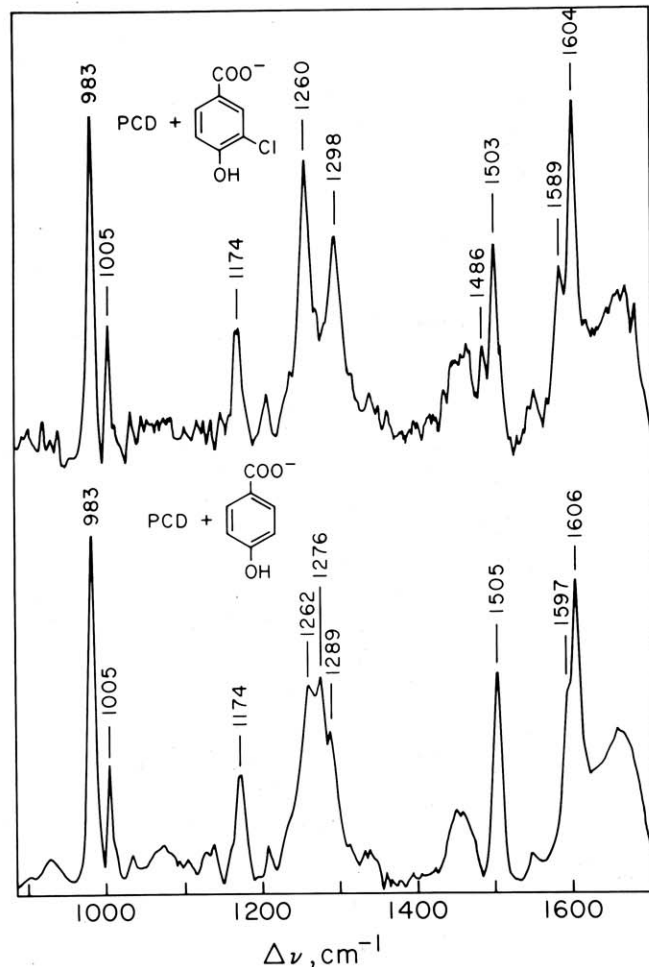


Figure 4. Resonance Raman spectra of PCD-inhibitor complexes (514.5 nm excitation).

spective transitions at a particular wavelength and the intensities are plotted as a function of wavelength. Figure 3 shows the excitation profile of  $\text{Fe}(\text{salen})(\text{OC}_6\text{H}_4\text{-}4\text{-CH}_3)$  and illustrates the relative energies of the salen-to-Fe(III) and the *p*-cresolate-to-Fe(III) charge-transfer transitions.

Resonance Raman studies on other dioxygenase complexes provide additional insights into the coordination chemistry of the iron center (19, 24, 25). Phenols, for example, are good inhibitors of the dioxygenases. Phenol binding results in a blue shift of the visible spectrum, indicating some structural alteration of the active site. Raman studies (Fig. 4) show that the inhibitor phenol coordinates to the iron center without displacing the endogenous tyrosinates. The coordination of the inhibitor is indicated by the presence of additional Raman features; these vary in energy as different phenols are introduced and are shifted by isotopic substitution. For example, the features at 1276 and 1597  $\text{cm}^{-1}$  shift upon ring deuteration of the 4-hydroxybenzoate in the PCD-4-hydroxybenzoate complex and are thus assigned to the inhibitor (24). Comparative studies on the PCD-3-chloro-4-hydroxybenzoate complex and the PCD-4-hydroxybenzoate complex indicate that two tyrosines are involved in coordinating the iron center (19, 24). The Raman spectrum of the former complex exhibits a  $\nu_{\text{C}-\text{O}}$  for the tyrosines which is approximately twice as intense as the  $\nu_{\text{C}-\text{O}}$  of the inhibitor phenol. Similarly, the PCD-4-hydroxybenzoate complex exhibits three nearly equally intense  $\nu_{\text{C}-\text{O}}$ 's, only one of which arises from the inhibitor. Thus the iron center is coordinated to two endogenous tyrosinates and has a site available for the coordination of exogenous ligands. The remaining ligands on the iron are proposed to be histidines (26) and water(or hydroxide) (27) to give rise to a five- or six-coordinate (28) metal center.

Substrate binding to the dioxygenases in the absence of oxygen results in the development of absorption in the long wavelength region (Fig. 1) (29, 30). The persistence of the visible spectrum suggests that the iron center is not reduced in this complex, as had been suggested earlier. Reduction of the iron center would have resulted in the bleaching the charge transfer band. EPR and Mossbauer studies corroborate the ferric nature of the iron in the enzyme-substrate (ES) complex (10–12). Raman studies on the ES complexes with 647.1 nm excitation (21) reveal new resonance-enhanced features at  $\sim$ 1260, 1320, and 1470  $\text{cm}^{-1}$ . These are due only to the substrate, as indicated by spectral shifts when ring-deuterated substrate is used. No tyrosinate vibrations are observed with 647.1 nm excitation in the ES complexes in contrast to parallel experiments on the native dioxygenases wherein they are observed (19). Based on this observation, one may suspect that catechol has coordinated to the iron center and displaced the tyrosines. However, when the excitation wavelength is shifted to 514.5 nm, both catecholate and tyrosinate vibrations are observed. Therefore, catecholate binding has the effect of shifting the tyrosinate-to-Fe(III) charge-transfer transition to higher energies.

A perusal of the various dioxygenase complexes reveals a spectrum of colors (31). The native enzymes are burgundy, phenol complexes are yellow-brown, carboxylate complexes are purple, thiophenol complexes are orange-brown, cyanide complexes are green, and substrate complexes are purplish gray. In all cases, the tyrosinate-to-Fe(III) charge-transfer band persists, as indicated by the presence of tyrosinate vibrations in the resonance Raman spectra of the complexes (19, 24, 25). These observations indicate that the charge-transfer transition is sensitive to the nature of the other ligands in the iron complex and that the charge-transfer band may be used to deduce the identity of an unknown ligand.

A systematic study on a series of  $\text{Fe}(\text{salen})\text{X}$  has investigated the factors that affect the energy of the phenolate-to-Fe(III) charge-transfer band (4). From a combination of observations from visible spectroscopy, paramagnetic NMR

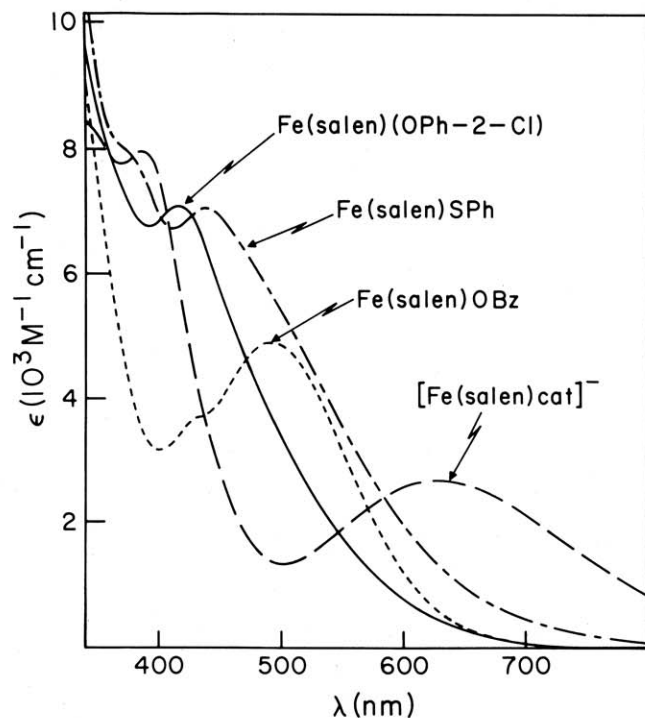


Figure 5. Visible absorption spectra of  $\text{Fe}(\text{salen})\text{X}$  complexes illustrating the shifts of the salen-to-Fe(III) charge-transfer band.

spectroscopy, Raman excitation profiles, and cyclic voltammetry measurements, it is concluded that the ligand field strength of X affects the energy of the charge transfer band; the better ligand X is, the higher the energy of the salen-to-Fe(III) charge transfer transition (Fig. 5). Based on these studies, a spectrochemical series has been developed.



The phenolate-to-Fe(III) charge-transfer transition shifts to higher energy as the series goes from left to right. This series will be useful in deducing the nature of the transient intermediates in the dioxygenase reaction.

The reaction of the dioxygenase ES complexes with dioxygen has been investigated with stopped-flow kinetics (32, 33). In most cases, two transient intermediates are observed and their rates of formation and decomposition can be calculated. From these rate constants, the visible spectra of the intermediates can be constructed; Figure 1 shows the spectra of the intermediates in the reaction of the PCD-protocatechuate complex with  $\text{O}_2$ . The sequence for the reaction is E, ES,  $\text{ESO}_2$ , and  $\text{ESO}_2^*$ . The native enzyme is obtained upon the decomposition of the second intermediate. Note that visible absorption remains in these intermediates, though the band shifts from one species to the next. This indicates the persistence of the tyrosinate-to-Fe(III) charge-transfer band as the exogenous ligand is transformed from substrate to product. The iron center would appear to be in the ferric state in these intermediates.

The observation of the ferric oxidation state in the native enzyme, the ES complex, and all the transient intermediates suggest the possibility that the iron does not undergo reduction during the catalytic cycle. Indeed the presence of tyrosines in the metal coordination environment serves to stabilize the ferric oxidation state (4) and has a profound effect on the mechanism of action for these enzymes.

Early mechanistic postulates required the binding of dioxygen to a ferrous center to serve as the oxygen activation step. Since the native enzyme was known to have a ferric center, it was proposed that substrate binding resulted in the

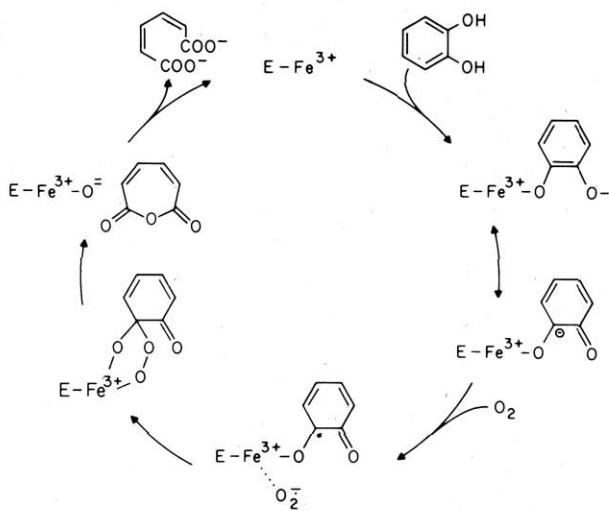


Figure 6. Proposed mechanism for the intradiol cleaving catechol dioxygenases.

reduction of the ferric center followed by oxygen binding and product formation. However, the spectroscopic data accumulated to date argues against such a mechanism, since the ES complexes are clearly ferric complexes. This data has forced a reevaluation of the proposed mechanism and has resulted in a different proposed mechanism, one which postulates that the ferric center activates the substrate for reaction with catechol (3). This mechanism is illustrated in Figure 6.

In the proposed mechanism, the substrate catechol is postulated to coordinate to the iron through only one oxygen. The coordinated substrate then acts as the reductant for oxygen, yielding as the substrate-oxygen adduct a peroxy species. The decomposition of the peroxy intermediate is then facilitated by coordination to the iron to yield an anhydride. The opening of the anhydride is effected by the metal-coordinated hydroxide. The opening of the anhydride is effected by the metal-coordinated hydroxide.

Perhaps the novel aspect of this mechanism is the mode of catecholate binding. Given the demonstrated affinity of catecholate for ferric ion (34), one would expect that the catecholate would chelate to the ferric center, as has been observed for several iron catecholate complexes. However, it is this stabilization due to chelation that one would want to avoid in order to obtain a reactive species. Support for the monodentate mode of catecholate coordination has been obtained from a paramagnetic NMR study of the CTD enzyme-substrate complexes (35).

Because of the presence of the high spin ferric center, proton resonances of ligands coordinated to the iron will be shifted out of the diamagnetic region. The ferric center in effect acts as an internal paramagnetic shift reagent in the protein. Since high spin ferric ion has a symmetric distribution of *d* electrons, the paramagnetic shift observed will arise only from a contact mechanism, i.e., delocalization of the unpaired spin density through bonds. Thus we may be able to distinguish between a monodentate and a chelated catecholate on the basis of NMR shift. For this one needs appropriate models. Such models have been synthesized (31) and their crystal structures (36, 37) are shown in Figure 7. Fe(saloph)catH is an example of a monodentate catechol complex, while K[Fe(salen)cat] is the corresponding chelated catecholate complex.

NMR spectra of the synthetic 4-methylcatecholate complexes are shown in Figure 8; 4-methylcatechol has been chosen as the probe substrate because the methyl-resonance is easily identified. From an analysis of the spectra, it is clear

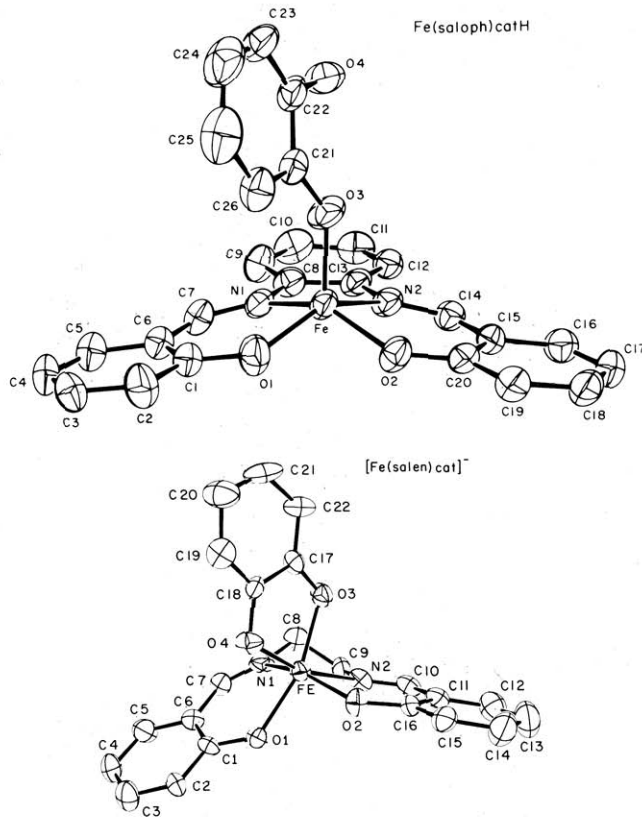


Figure 7. ORTEP plots of the crystal structures of Fe(saloph)catH and K[Fe(salen)cat].

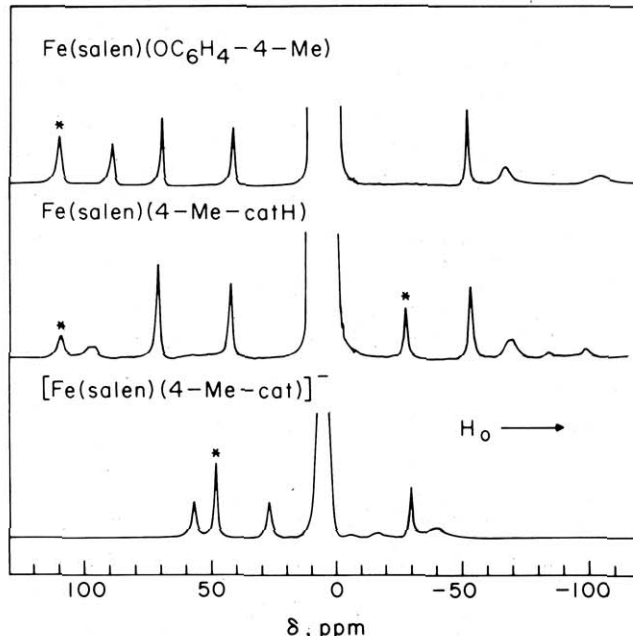
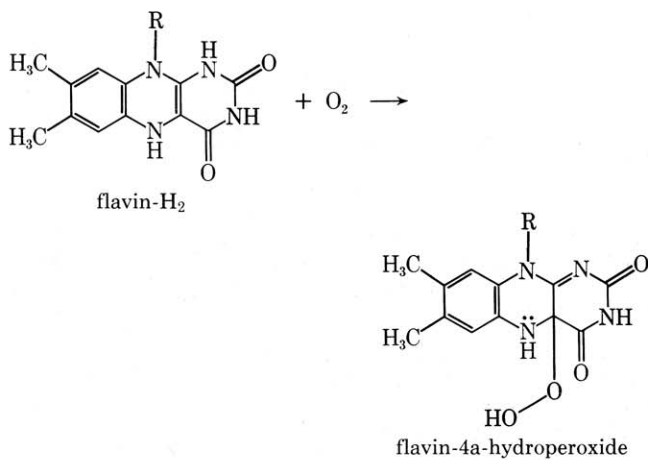


Figure 8. Paramagnetic  $^1\text{H}$ -NMR spectra of Fe(salen) complexes in acetone- $d_6$ . Starred resonances are assigned to the  $\text{CH}_3$  group.

that the different modes of catecholate binding can be distinguished by this technique (31). For monodentate catecholates, the methyl resonance appears at  $\sim 100$  ppm downfield if the O-1 oxygen were coordinated to the iron and at  $\sim 30$  ppm upfield if the O-2 oxygen were coordinated. The same shifts are observed for methyl-substituted phenols. For chelated catecholates, the methyl resonance appears at  $\sim 50$

ppm downfield. The NMR spectra of CTD ES complexes are shown in Figure 9. Comparisons of the spectrum of the CTD-catechol complex with that of the CTD-4-methylcatechol complex show the principal difference in the two spectra is a new feature in the latter at 100 ppm downfield. This peak disappears in the  $^1\text{H}$ -spectrum when 4-(methyl- $d_3$ )-catechol is used as substrate and is observed in the corresponding  $^2\text{H}$ -NMR spectrum. The data clearly indicate that the substrate is coordinated to the ferric center solely through the O-1 oxygen (35).

The subsequent aspects of the mechanism have precedents in the bioorganic literature. The formation of the peroxy intermediate is analogous to the reaction of reduced flavin with oxygen to form the 4a-hydroperoxide (38), i.e.,



This peroxy species may be the first intermediate observed in the stopped-flow studies (ESO<sub>2</sub> in Fig. 1). The blue shift of the charge transfer band would be consistent with the coordination of the peroxy to the ferric ion, since the alkyl peroxy would have a basicity similar to that of phenolate. The rearrangement of the peroxy intermediate to the desired product can occur via the anhydride as shown or via a dioxetane (39). The formation of the anhydride would be a result of a Crigee rearrangement (e.g., Baeyer-Villiger reaction), while the dioxetane is similar to intermediates in chemiluminescent reactions (40). For CTD, the intermediacy of the anhydride has been demonstrated by  $^{18}\text{O}$ -labeling experiments (41).

The remaining challenge for the bioinorganic chemist in this work is the duplication of this reaction in a small molecule. Progress toward a model iron complex capable of catalyzing this reaction has been encouraging. The initial reactivity studies on the Fe(salen)catecholate complexes proved disappointing (42). Though the monodentate complex was oxidized by dioxygen and the chelated complex was unreactive, as suggested by the proposed mechanisms, the reactivity observed was simply a one-electron oxidation to a semi-quinone complex. More recent results show that a ligand system like the tripodal NTA (nitrilotriacetic acid) is more effective. Weller and Weser have demonstrated that Fe(NTA) in an organic solvent-buffer mixture catalyzes the oxidative cleavage of 3,5-di-*tert*-butylcatechol (DBC) in 80% yield based on substrate with as many as 100 turnovers (43). Crystals of [Fe(NTA)DBC]<sup>2-</sup> show a six-coordinate complex with the catecholate unsymmetrically chelated to the iron center (Fig. 10) (44). The Fe-O (DBC) bond trans to N is 1.89 Å, 0.09 Å shorter than the other Fe-O(DBC) bond; this is ascribed to the weakness of the Fe-N bond which is compensated by the stronger Fe-O(DBC) bond trans to it. This complex reacts with O<sub>2</sub> in DMF over a period of four days to yield cleavage product in 80% yield.  $^{18}\text{O}$  studies show a very clean incorporation of a single oxygen label, strongly in support of an anhydride intermediate. The reactivity of the complex is proposed to result from the breaking of the weak-

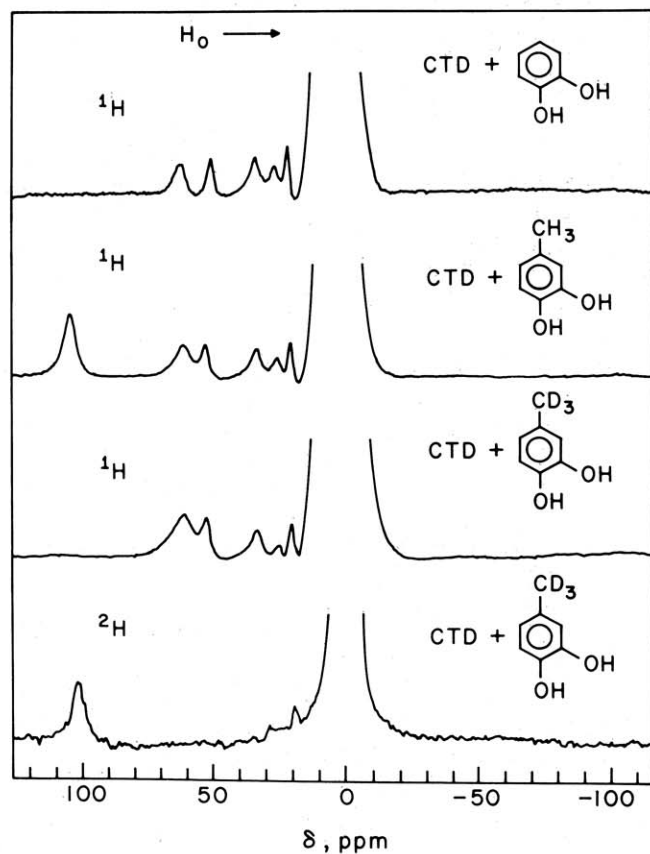
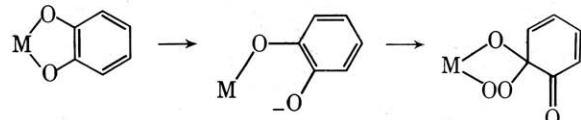


Figure 9. Paramagnetic  $^1\text{H}$ -NMR spectra of catechol 1,2-dioxygenase ES complexes.

er Fe-O(DBC) bond generating the reactive monodentate catecholate complex.



The rate of the reaction is consistent with the high activation energy necessary to break the Fe-O(DBC) bond. Despite the slow rate of this reaction, it is clear that the enzyme chemistry can be mimicked in a synthetic system. It is hoped that this discussion has served to demonstrate the various approaches required to unravel the details of the structure and mechanism of a metallo-enzyme.

#### Acknowledgments

This work was supported by the National Institutes of Health, the Alfred P. Sloan Foundation, and the University of Minnesota Graduate School Research Fund. The research described is the result of the accumulated efforts of R. H. Heistand, II, R. B. Lauffer, R. J. Mayer, A. L. Roe, L. S. White, and J. W. Pyrz, to whom I am most grateful.

#### Literature Cited

- (1) Que, L., Jr., *Adv. Inorg. Biochem.*, **5**, 167 (1983).
- (2) Feist, C. T., and Hegeman, G. D., *J. Bacteriol.*, **100**, 1121 (1969); Ornsten, L. N., and Stanier, R. Y., *J. Biol. Chem.*, **241**, 3776 (1966).
- (3) Que, L., Jr., Lipscomb, J. D., Munck, E., and Wood, J. M., *Biochim. Biophys. Acta*, **485**, 60 (1977).
- (4) Pyrz, J. W., Roe, A. L., Stern, L. J., and Que, L., Jr., *J. Amer. Chem. Soc.*, **107**, 614 (1985).
- (5) Hayashi, O., Katagiri, M., and Rothberg, S., *J. Amer. Chem. Soc.*, **77**, 5450 (1955).
- (6) Nakai, C., Kagamiyama, H., Saeki, Y., and Nozaki, M., *Arch. Biochem. Biophys.*, **195**, 12 (1979).
- (7) Iwaki, M., Kagamiyama, H., and Nozaki, M., *J. Biochem. (Tokyo)*, **86**, 1159 (1979); Iwaki, M., Kagamiyama, H., and Nozaki, M., *Arch. Biochem. Biophys.*, **210**, 210 (1981).

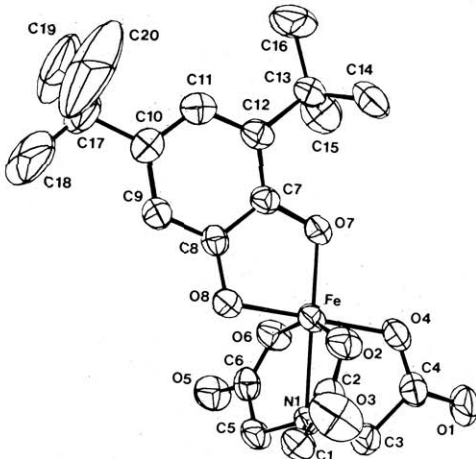


Figure 10. ORTEP plot of the crystal structure of  $[Fe(NTA)DBC]^{2-}$  (NTA, nitrilotriacetic acid; DBC, 3,5-di-*tert*-butyl-catecholate dianion).

- (8) Kohlmiller, N. A., and Howard, J. B., *J. Biol. Chem.*, **254**, 7302 (1979); Kohlmiller, N. A., and Howard, J. B., *J. Biol. Chem.*, **254**, 7309 (1979).
- (9) Satyshur, K. A., Rao, S. T., Lipscomb, J. D., and Wood, J. M., *J. Biol. Chem.*, **255**, 10015 (1980).
- (10) Que, L., Jr., Lipscomb, J. D., Zimmerman, R., Munck, E., Orme-Johnson, N. R., and Orme-Johnson, W. H., *Biochim. Biophys. Acta*, **452**, 320 (1976).
- (11) Whittaker, J. W., Lipscomb, J. D., Kent, T. A., and Munck, E., *J. Biol. Chem.*, **259**, 4466 (1984).
- (12) Kent, T. A., Munck, E., Whittaker, J. W., Lipscomb, J. D., Que, L., Jr., unpublished observations.
- (13) Oosterhuis, W. T., *Struct. Bond. (Berlin)*, **20**, 59 (1974).
- (14) Nakazawa, T., Kojima, Y., Fujisawa, H., Nozaki, M., Hayaishi, O., and Yamano, T., *J. Biol. Chem.*, **240**, PC3224 (1965).
- (15) Fujisawa, H., Uyeda, M., Kojima, Y., Nozaki, M., and Hayaishi, O., *J. Biol. Chem.*, **247**, 4414 (1972).
- (16) Blumberg, W. E., and Peisach, J., *Ann. N.Y. Acad. Sci.*, **222**, 539 (1973).
- (17) Tatsuno, Y., Saeki, Y., Iwaki, M., Yagi, T., Nozaki, M., Kitagawa, T., and Otsuka, S., *J. Amer. Chem. Soc.*, **100**, 4614 (1978).
- (18) Keyes, W. E., Loehr, T. M., and Taylor, M. L., *Biochem. Biophys. Res. Comm.*, **83**, 941 (1978).
- (19) Felton, R. H., Cheung, L. D., Phillips, R. S., and May, S. W., *Biochem. Biophys. Res. Comm.*, **85**, 844 (1978).
- (20) Bull, C., Ballou, D. P., and Salmeen, I., *Biochem. Biophys. Res. Comm.*, **87**, 836 (1979).
- (21) Que, L., Jr., Heistand, R. H., II, *J. Amer. Chem. Soc.*, **101**, 2219 (1979).
- (22) Tomimatsu, Y., Kint, S., and Scherer, J. R., *Biochemistry*, **15**, 4918 (1976).
- (23) Yachandra, V. K., Hare, J., Moura, I., and Spiro, T. G., *J. Amer. Chem. Soc.*, **105**, 6455 (1983).
- (24) Que, L., Jr., and Epstein, R. M., *Biochemistry*, **20**, 2545 (1981).
- (25) Que, L., Jr., Heistand, R. H., II, Mayer, R., and Roe, A. L., *Biochemistry*, **19**, 2588 (1980).
- (26) Felton, R. H., Barrow, W. L., May, S. W., Sowell, A. L., Goel, S., Bunker, G., Stern, E. A., *J. Amer. Chem. Soc.*, **22**, 6132 (1982).
- (27) Whittaker, J. W., and Lipscomb, J. D., *J. Biol. Chem.*, **259**, 4487 (1984).
- (28) Roe, A. L., Schneider, D. J., Mayer, R., Pyrz, J. W., Widom, J., and Que, L., Jr., *J. Amer. Chem. Soc.*, **106**, 1676 (1984).
- (29) Kojima, Y., Fujisawa, H., Nakazawa, A., Nakazawa, T., Kanetsuna, F., Taniuchi, H., Nozaki, M., and Hayaishi, O., *J. Biol. Chem.*, **242**, 3270 (1967).
- (30) Fujisawa, H., and Hayaishi, O., *J. Biol. Chem.*, **243**, 2673 (1968).
- (31) Heistand, R. H., II, Lauffer, R. B., Fikrig, E., and Que, L., Jr., *J. Amer. Chem. Soc.*, **104**, 2789 (1982).
- (32) Bull, C., Ballou, D. P., and Otsuka, S., *J. Biol. Chem.*, **256**, 12681 (1981).
- (33) Walsh, T. A., Ballou, D. P., Mayer, R., and Que, L., Jr., *J. Biol. Chem.*, **258**, 14422 (1983).
- (34) Raymond, K. N., Isied, S. S., Brown, L. D., Fronczeck, F. R., and Nibert, J. H., *J. Amer. Chem. Soc.*, **98**, 1767 (1975).
- (35) Lauffer, R. B., and Que, L., Jr., *J. Amer. Chem. Soc.*, **104**, 7324 (1982).
- (36) Heistand, R. H., II, Roe, A. L., and Que, L., Jr., *Inorg. Chem.*, **21**, 676 (1982).
- (37) Lauffer, R. B., Heistand, R. H., II, and Que, L., Jr., *Inorg. Chem.*, **22**, 50 (1983).
- (38) Walsh, C. T., "Enzymatic Reaction Mechanisms," Freeman, San Francisco, 1977, pp. 390, 413.
- (39) Hamilton, G. A., in "Molecular Mechanisms of Oxygen Activation" (Editor: Hayaishi, O.), Academic Press, New York, 1974, p. 405.
- (40) Hiatt, R., in "Organic Peroxides," Vol. II, (Editor: Swern, D.), Wiley Interscience, New York, 1971, p. 1.
- (41) Mayer, R. J., and Que, L., Jr., *J. Biol. Chem.*, **259**, 13056 (1984).
- (42) Lauffer, R. B., Heistand, R. H., II, and Que, L., Jr., *J. Amer. Chem. Soc.*, **103**, 3947 (1981).
- (43) Weller, M. G., and Weser, U., *J. Amer. Chem. Soc.*, **104**, 3752 (1982).
- (44) White, L. S., Nilsson, P. V., Pignolet, L. H., and Que, L., Jr., *J. Amer. Chem. Soc.*, **106**, 8312 (1984).